AGU PUBLICATIONS

Space Weather

RESEARCH ARTICLE
10.1002/2016SW001381

Key Points:
- We compare noise from LRO LOLA SiAPDs with radiation measurements from the onboard CRaTER instrument
- We did not find evidence to support radiation as the cause of changes in detector noise
- The 1.3 cm Ti and Be shielding of the LOLA SiAPDs may be sufficient for interplanetary missions

Correspondence to:
E. B. Clements,
eclements@mit.edu

Citation:
Clements, E. B., A. K. Carlton, C. J. Joyce, N. A. Schwadron, H. E. Spence, X. Sun, and K. Cahoy (2016), Interplanetary space weather effects on Lunar Reconnaissance Orbiter avalanche photodiode performance, *Space Weather*, *14*, doi:10.1002/2016SW001381.

Received 1 MAR 2016
Accepted 23 APR 2016
Accepted article online 2 MAY 2016

Interplanetary space weather effects on Lunar Reconnaissance Orbiter avalanche photodiode performance

E. B. Clements[1], A. K. Carlton[1], C. J. Joyce[2], N. A. Schwadron[2], H. E. Spence[2], X. Sun[3], and K. Cahoy[1]

[1]Department of Aeronautics and Astronautics, Massachusetts Institute of Technology, Cambridge, USA, [2]Institute for the Study of Earth, Oceans, and Space (EOS), University of New Hampshire, Durham, New Hampshire, USA, [3]NASA Goddard Space Flight Center, Greenbelt, Maryland, USA

Abstract Space weather is a major concern for radiation-sensitive space systems, particularly for interplanetary missions, which operate outside of the protection of Earth's magnetic field. We examine and quantify the effects of space weather on silicon avalanche photodiodes (SiAPDs), which are used for interplanetary laser altimeters and communications systems and can be sensitive to even low levels of radiation (less than 50 cGy). While ground-based radiation testing has been performed on avalanche photodiode (APDs) for space missions, in-space measurements of SiAPD response to interplanetary space weather have not been previously reported. We compare noise data from the Lunar Reconnaissance Orbiter (LRO) Lunar Orbiter Laser Altimeter (LOLA) SiAPDs with radiation measurements from the onboard Cosmic Ray Telescope for the Effects of Radiation (CRaTER) instrument. We did not find any evidence to support radiation as the cause of changes in detector threshold voltage during radiation storms, both for transient detector noise and long-term average detector noise, suggesting that the approximately 1.3 cm thick shielding (a combination of titanium and beryllium) of the LOLA detectors is sufficient for SiAPDs on interplanetary missions with radiation environments similar to what the LRO experienced (559 cGy of radiation over 4 years).

1. Introduction

Radiation from solar activity or galactic cosmic rays can harm satellites, especially interplanetary spacecraft which must leave the protection of Earth's magnetic field. For example, the Halloween solar storms of 2003 are believed to have affected at least 28 satellites [*Webb and Allen*, 2004].

Space weather events can cause high fluxes and doses of radiation, which can have several effects on space systems, including single event upsets, deep dielectric discharges, surface charging, and total dose effects [*Hastings and Garrett*, 1996; *Baker*, 2000].

The response of avalanche photodiodes (APDs) to space weather is critical to understand and to quantify due to their common use on space missions for laser altimeters and lidar [*Sun et al.*, 2013] and their high sensitivity to radiation. Several NASA missions carry APDs, including the Lunar Reconnaissance Orbiter (LRO) [*Chin et al.*, 2007], the MErcury Surface, Space ENvironment, GEochemistry, and Ranging (MESSENGER) spacecraft [*Sun and Neumann*, 2015], and the Mars Global Surveyor [*Smith et al.*, 2001], [*McGarry et al.*, 1991]. Organizations other than NASA are also pursuing space-based laser altimeter projects. APDs are very sensitive to noise from radiation, which can interfere with instrument performance. For example, a single photon counting Geiger mode APD on the Ice, Cloud, and land Elevation Satellite (ICESat) launched in January 2003 was clearly affected by the Halloween storms: dark current rates rose from a prestorm average of 30 counts/s to 3800 counts/s during the three day storm period (28–30 October 2003) [*Sun et al.*, 2004].

The LRO was launched in 2009 and carried several scientific instruments. The two of interest for this paper are the Lunar Orbiter Laser Altimeter (LOLA) [*Smith et al.*, 2010] and the Cosmic Ray Telescope for the Effects of Radiation (CRaTER) [*Spence et al.*, 2010]. The relative locations of the two instruments are shown in Figure 1 and a more detailed view of the LOLA instrument is shown in Figure 2. Sensor data from the onboard CRaTER instrument are compared with the LOLA silicon avalanche photodiode detector (SiAPD) noise measurements in the form of threshold voltage to provide an improved measurement of SiAPD radiation sensitivity.

Figure 1. LRO spacecraft with the LOLA and CRaTER instruments identified. Image provided by X. Sun, NASA Goddard Space Flight Center. See *Ramos-Izquierdo et al.* [2009] for related images.

1.1. Radiation Sensitivity of Avalanche Photodiodes

Avalanche photodiodes can be affected by radiation in two ways: in the short term, the high energy of the radiation event can cause additional noise in the detector, while in the long term, radiation can damage the detector and cause noisier readings even after the end of the solar storm. Traditional photodiodes generate

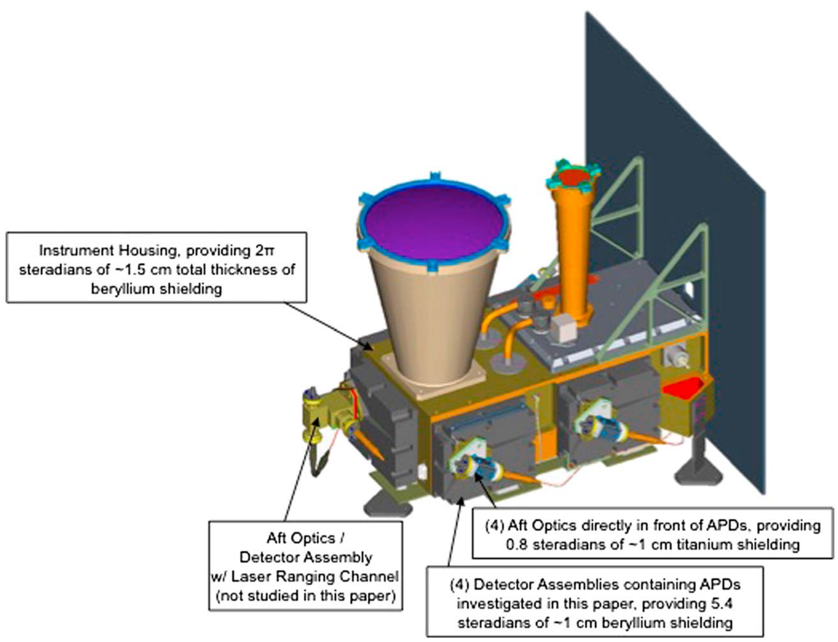

Figure 2. LOLA with detector assemblies and approximate shielding labeled. Note that the detector is under a folded optical path, so the shielding is larger than it may be in similar systems. The shielding is estimated based on averaging of shielding from different angles through the surrounding material. Computer Aided Design (CAD) image provided by X. Sun, NASA Goddard Space Flight Center. See *Ramos-Izquierdo et al.* [2009] for related images.

current when photons hit the detector and create an electron-hole pair. APDs have an additional property that creation of the electron-hole pair causes the formation of more electron-hole pairs in an electron avalanche effect. Therefore, APDs are more sensitive to radiation (lower threshold particle fluxes and energies) than traditional photodiodes [*Wegrzecka et al.*, 2004] and could show sensitivity to radiation events in the form of increased noise levels like ICESat did during the 2003 Halloween Solar Storms. The sensitivity of APDs is affected by whether or not they are operated in Geiger mode, which represents several orders of magnitude increase in avalanche gain. In linear mode, the APD output is proportional to the incident optical power. In Geiger mode, the APD is biased above the breakdown voltage and avalanche breakdown can be triggered by internal dark current electrons or incident photons [*Laforce*, 2009]. With a proper quenching circuit that restores the bias to the APD after an avalanche breakdown, a Geiger mode APD can be used to count single photon events. Because the response to solar storms reported by ICESat was from Geiger mode SiAPDs, while this paper examines the response of linear mode SiAPDs to solar storms, studying the response of LOLA's SiAPDs to radiation is of use to the community.

The LOLA detectors are protected by titanium housing around each of the five detectors, which is mounted to a beryllium structure, totalling approximately 1.3 cm thick shielding (combination of titanium and beryllium) [*Ramos-Izquierdo*, 2007], [*Ramos-Izquierdo et al.*, 2009]. The arrangement of the shielding is shown in Figure 2. This provides roughly a factor of 10^3 reduction in total dose radiation based on a simple radiation model of a 1.3 cm finite aluminum slab using ESA's Space Environment Information System (SPENVIS) [*Kruglanski*, 2015]. While SPENVIS does not have data to support shielding simulations of titanium or beryllium, linear energy transfer (LET) is proportional to material density [*Tavernier*, 2010], so the expected LET from aluminum is roughly half of the expected LET for the titanium housing. We note that the APDs, as optical instruments, have windows. However, the optical path shown in *Ramos-Izquierdo et al.* [2009, Figure 5] is folded, acting as additional shielding to the detector.

2. Measurement Description

We analyze noise data from the LOLA instrument and compare changes in the noise data with dose data from the CRaTER instrument. Noise in the LOLA instrument is caused by sources internal to the instrument (e.g., dark current), spacecraft operations, and the environment (e.g., sunlight or radiation), so determining the effects of radiation on SiAPD noise requires disentangling the effects of these other sources. In this section, we describe the LOLA instrument, including the various sources of noise, and the CRaTER instrument.

2.1. SiAPD Noise Data From the LOLA Instrument

LOLA is a laser altimeter used for mapping the height of the lunar surface. LOLA carries five silicon avalanche photodiode detectors (SiAPDs). Detectors 2 through 5 are used to receive the pulses reflected from the lunar surface, and these are the focus of our analysis. Detector 1 is used to receive pulses from Earth-directed laser ranging in addition to laser pulses reflected from the lunar surface, so it is excluded from this analysis.

The APD noise data consist of threshold voltage measurements which may be affected by space weather events as the ICESat APD was during the 2003 Halloween storms. Possible effects include long-term drift of the threshold voltage due to total dose and short-term spikes in noise counts due to high energy particle flux events.

The LOLA noise data used in this study are the detector threshold voltage, which is automatically adjusted up or down to maintain a constant false alarm probability in the detector system [*Barker et al.*, 2015a, 2015b]. These noise counts are a combination of dark noise from the detector itself, shot noise from the background light illumination, and noise in the preamplifier circuit. Thus, a small change in the threshold actually corresponds to a large photocurrent change. In this report, we study the possibility of an additional source of noise from space weather events by determining the noise from traditional sources and inferring the excess noise.

We consider only data from September 2009 to October 2013. Beginning in November 2013, the instrument was often used in passive mode and the threshold voltage was lowered for this mode. Therefore, the data from this later time period cannot be directly compared with previous data.

2.1.1. Sources of Noise Unrelated to Space Weather

Noise can be caused by intrinsic dark current or by unwanted photons from sources other than the reflected laser pulse entering the detector. Mission operations can affect either of these noise sources.

Table 1. LRO/LOLA Mission Timeline

Event	Date/Frequency
Launch	18 June 2009
LOLA continuous data collection begins	July 2009
Nominal operations	September 2009
Transition to science mission	September 2010
Transition to extended science mission	September 2012
Station-keeping maneuvers	Monthly
Thermal blanket causing laser beam expander misalignment	Every eclipse period
Spacecraft in full sun, long duration	Twice per year
Spacecraft day/night cycle	48 min each orbit

Noise in the preamplifier circuit may be caused by spacecraft actions unrelated to the SiAPDs, such as maneuvers or other state changes. Significant mission events and periodic actions lead to noise anomalies unrelated to space weather events. Table 1 shows the mission time line and periodic actions. This information was obtained from *Mazarico et al.* [2012].

2.2. The CRaTER Instrument

In situ measurements of the deep space radiation environment near the LOLA SiAPDs are provided by the CRaTER experiment on the LRO, which measures the effects of ionizing energy loss in matter due to solar energetic particles and galactic cosmic rays [*Spence et al.*, 2010]. Furthermore, we note that though LRO measurements are made near the Moon, which is itself a source of secondary ionizing radiation, *Spence et al.* [2013] showed that greater than 90% of the CRaTER dose is from primary cosmic rays, meaning that results obtained in lunar orbit are excellent proxies for deep space radiation conditions.

The CRaTER instrument is comprised of silicon solid-state detectors designed to measure the linear energy transfer (LET) spectrum, particularly the interactions of higher energy ions (>10 MeV). Therefore, the CRaTER experiment is well suited for a comparison to the LOLA noise data.

The CRaTER Analog Processing Board (APB) contains a device for measuring the total radiation dose experienced by the electronics on the APB. The device provides mRad (0.01 mGy) resolution and full scale reading of 335 rad (3.35 Gy). For more information on how dose deposited in the silicon detectors (CRaTER detectors D1 and D2) is measured, see *Schwadron et al.* [2012]. The CRaTER dose data were compared to an onboard microdosimeter, providing uncertainty measurements of galactic cosmic rays and solar energetic particles of 15% [*Schwadron et al.*, 2012]. While the LET is likely lower for the LOLA SiAPDs than for the CRaTER instrument, we expect the events detected in the LOLA results to having a corresponding response from the CRaTER instrument.

3. Analysis

Starting with the raw LOLA SiAPD threshold voltage noise data, our analysis approach is to remove noise that can be accounted for by sources other than solar storms and then compare the remaining noise data with CRaTER accumulated dose data. We consider the removal of noise from

1. *Sunlight*. We considered only noise data from nighttime measurements, which would remove the noise effects of sunlight (as LOLA is always facing the moon when operating, sunlight comes from reflection off the moon's surface).
2. *LRO Orbit and Mission Operations*. We used data from the periods of full moons, when the LRO's eclipse period is darkest (light reflecting off the Earth is not visible).
3. *Radiation shielding provided by the Moon*. A previous study by the CRaTER instrument team found significant correlation between the orbit altitude of the LRO and the radiation dose seen [*Mazur et al.*, 2011]. We coplotted the data resulting from 1 and 2 with the LRO orbit to identify when orbit changes relate to noise changes.

After the removal of known noise, we consider that the remaining noise may be due to space weather events and may be a measurement of such space weather events. Then, the remaining noise is compared with the

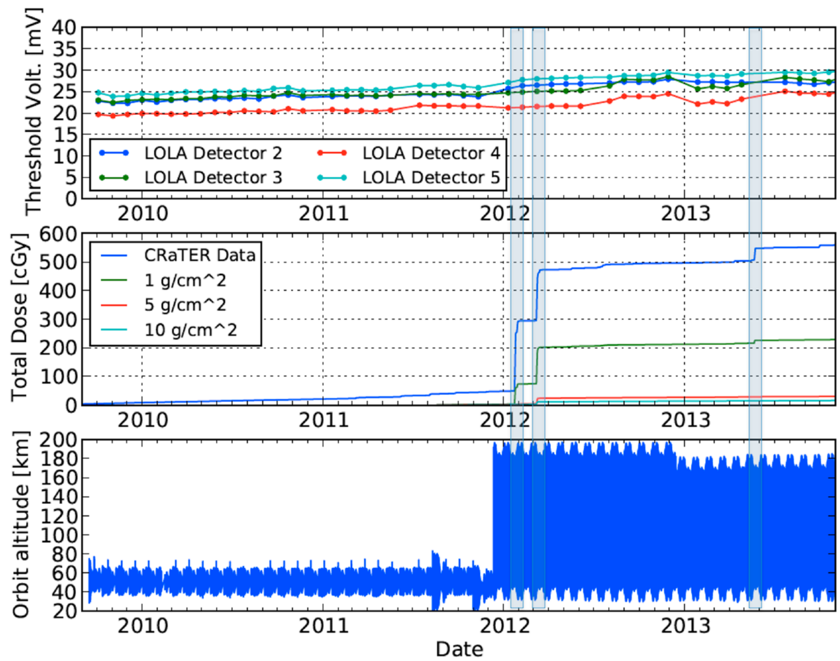

Figure 3. Lunar Month Average Eclipse Threshold Voltage compared with CRaTER data from the D1 and D2 detectors and estimated radiation dose for 1, 5, and 10 g/cm^2 of shielding. CRaTER data (center subplot) shows storms during January 2012, and May 2013, highlighted in blue. The 2012 and 2013 solar storms occurred during gentle increases in threshold voltage. Differences between data points during solar storms are shown are listed in Table 2 and long-term drift estimates are shown in Table 3.

accumulated dose data from the CRaTER instrument through statistical correlations, which are described in section 3.1.

3.1. Comparison With CRaTER Data

We plot the resulting data with the CRaTER measurements of accumulated dose from the D1 and D2 detectors. Three periods of the CRaTER data in the time period under study show notable increases in total dose: January 2012, March 2012, and May 2013. We then focused on those time periods in the LOLA eclipse threshold voltage and compared the average eclipse threshold voltage during the full moon eclipses before and after each period.

4. Results

In this section the long-term effects of radiation are quantified by calculating the percentage change in the average eclipse threshold voltage during the darkest part of each month before and after each solar storm. The short-term effects of radiation are investigated by plotting the eclipse threshold voltage (without monthly

Table 2. Comparison of the Increases in Total Dose During Each Solar Storm With Percent Change in Average Eclipse Threshold Voltage During Darkest Eclipses[a]

	Average	Jan 2012	Mar 2012	May 2013
Δ Total Dose (cGy)		245	17.9	34.0
Δ Dose with 5 g/cm^2		0.78	19.5	0.68
Detector 2	1.13%	2.5%	0.5%	0.016%
Detector 3	1.61%	0.7%	0.7%	6.6%
Detector 4	1.74%	0.7%	0.9%	7.9%
Detector 5	1.17%	2.5%	0.7%	1.3%

[a]The first column gives the average change between months, while the other columns show the changes during solar storms. Contents of table are based on differences between data points shown in Figure 3.

Table 3. Percent Change in Average Eclipse Threshold Voltage During Darkest Eclipses Over Four Years[a]

	Change Sep 2009–Oct 2013
Total dose (cGy)	559
Detector 2	19%
Detector 3	19%
Detector 4	24%
Detector 5	19%

[a]Contents of table are based on differences between data points shown in Figure 3.

averaging) versus the dose rate for each major solar storm in Figure 5. A comparison of the threshold voltage with the accumulated radiation dose from the CRaTER data does not indicate solar storms had severe effects on SiAPD noise, as shown in Figures 3 and 5. While there is a steady increase in threshold voltage over the period from 2010 to late 2013 that could be caused by radiation dose, the rate of threshold voltage change does not correlate with the periods of highest radiation.

4.1. Long-Term Effects of Radiation on SiAPD Noise

The long-term drift in threshold voltage does not appear to be affected by the solar storms measured by CRaTER, as illustrated in Figure 3. The percent change in the data points in Figure 3 resulting from the solar storms of January 2012, March 2012, and May 2013 are given in Table 2. Of these events, the January 2012 per- T2
cent change in threshold voltage was the smallest, despite this storm having the largest total dose increase. Because the dose experienced by the LOLA SiAPDs is affected by the shielding in the direction of the incoming radiation, we plot estimated doses for different shielding levels in Figure 3 and include an estimated reduced dose for the nominal shielding thickness in Table 2. The multiple curves are necessary because the exact amount of shielding around the detector varies spatially and the direction of the incoming radiation is not well known. The cumulative drift in threshold voltage over the 3 years under study is given in Table 3. Additionally, Figure 4 shows a comparison of the monthly percent change in threshold voltage with the increase in radiation for a given month and illustrates that the changes during solar storms were not unusual for these detectors. Based on these results, a half inch of titanium shielding around SiAPD detectors appears to provide sufficient protection.

4.2. Short-Term Effects of Radiation on SiAPD Noise

We investigated the short-term effects of radiation on LOLA noise by plotting the threshold voltage during each solar storm as well as the dose rate, as shown in Figure 5. For two of the three solar storms, the threshold voltage did not appear to have any short-term spikes when the radiation dose rate was highest. The exception was one peak during the January 2012 event, but this peak is similar to other peaks from that time period that did not occur during radiation storms so it appears to be coincidental. Additionally, while CRaTER data

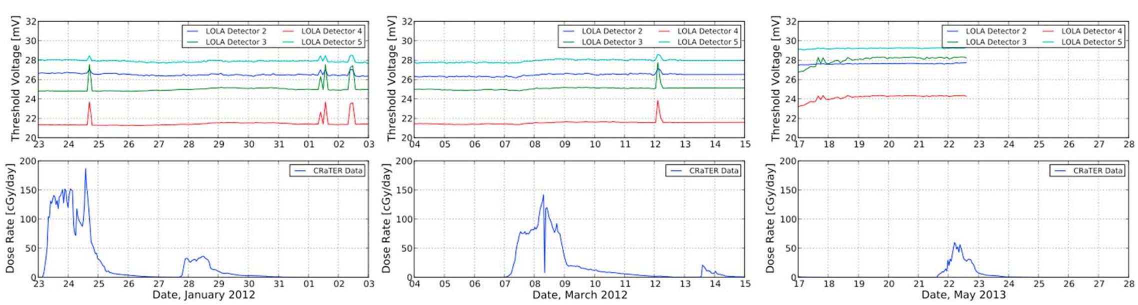

Figure 4. Orbital average eclipse threshold voltage shows little variation during the periods of highest dose rate measured by the CRaTER instrument using the D1 and D2 detectors. While averaging smooths the data, the periods of higher radiation extended much longer than the periods of averaging. In January 2012, a peak in threshold voltage happens to occur during a radiation storm, but similar peaks occur at other times such as 1 and 2 February, so this not thought to be related to space weather. While it is possible the January peak was due to the particularly high dose rate at that time, we cannot disprove that the peak was a coincidence given the similar peaks on 1 and 2 February. The eclipse threshold voltage pauses at 22 May 2013 because the spacecraft entered its biannual period of extended full sunlight as described in Table 1.

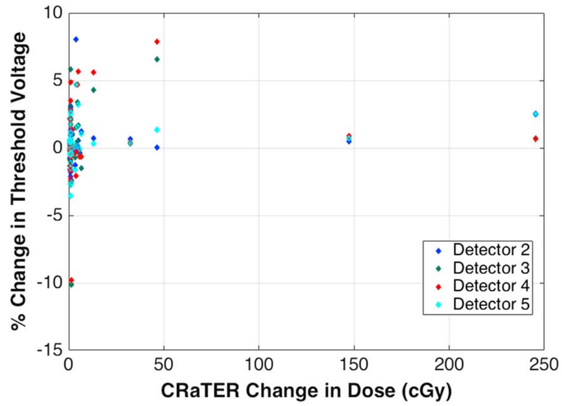

Figure 5. A comparison of changes in threshold voltage from month to month of the data points shown in Figure 3 shows that the increases in threshold voltage do not increase with increasing radiation doses.

are sensitive to low and high energies, we also examined proton flux data explicitly at seven energies (2.5, 6.5, 11.6, 30.6, 63.1, 165.0, and 433.0 MeV) using the Earth-Moon-Mars Radiation Environment Module (EMMREM) [*Schwadron et al.*, 2010], used to describe the radiation environment in lunar orbit. We find no relationship between the EMMREM measurements and the LOLA threshold voltage events beyond the events already detected by the CRaTER instrument.

4.3. Comparison With Ground Measurements

The validation of the LOLA analysis has two parts: validation of the measured detector response to radiation and validation of the measured radiation.

Prior to launch, qualification models of the LOLA detectors have been tested with two forms of radiation—gamma radiation and proton radiation. According to *Sun et al.* [1997], gamma radiation of 200 keV did not yield SiAPD performance degradation. However, while gamma rays do cause the same amount of ionization damage as protons, they do not cause the same displacement damage (X. Sun, personal communication, 2012).. Therefore, proton testing was also done on the SiAPDs. This testing showed that doses of 2 Gy (without shielding) were sufficient to cause 5–20% changes in average dark counts. Individual solar storms measured by CRaTER were of similar energy levels to the 2 Gy from ground testing, with a maximum of 2.45 Gy in an individual solar storm as shown in Table 2. The low response of the detectors during these storms (less than 2.5% change in threshold voltage during the largest storm) suggests the shielding was effective in reducing the dose, as predicted in section 1.1.

5. Conclusion

This work compares the threshold voltage noise readings from silicon avalanche photodiodes (SiAPDs) on the LRO LOLA instrument with radiation dose data from the LRO CRaTER instrument. Both long-term LOLA SiAPD damage and transient SiAPD noise effects were investigated and neither appeared to be significantly affected by solar storms measured by the CRaTER instrument. The threshold voltage exhibited a 18–23% increase over the 3 years under study, but the rate of change did not increase during storms.

While the LOLA APDs did not show a response both in the short and long term, the radiation events since LRO launched in mid-2009 are not representative of the extremes future SiAPDs could face. The largest events LOLA SiAPDs saw had a peak of 10 MeV flux at 6310 pfus (particle flux units) for the January 2012 event and 6530 pfus for the March 2012 event. The May 2013 event had a peak flux of 1660 pfus. While the LOLA SiAPDs did not show a response to the events since LRO was launched in mid-2009, the Halloween event in 2003 that affected the ICESat APDs, for example, had a peak of 29,500-pfus, about 5 times higher than the 2012 events. Other events over the past two decades have reached particle fluxes even greater than the Halloween storms in 2003 (e.g., 31,700 pfus in November 2001, 40,000 pfus in October 1989, and 43,000 pfus in March 1991). Therefore, while 1.3 cm of Ti and Be has been sufficient shielding for the LOLA APDs, this conclusion is unproven for extreme lunar radiation environments. In summary, the data suggest that the 1.3 cm of Ti and Be of shielding for LOLA is sufficient for SiAPDs outside of the protection of the Earth's magnetosphere, even for highly sensitive lidar instruments such as LOLA, on long-term missions with expected radiation doses similar to the LRO mission (559 cGy of radiation over 4 years), but care should be taken in assuming that larger storms would not affect future missions.

Acknowledgments
E.B.C. was funded by the MIT Lincoln Laboratory Lincoln Scholars Program. C.J.J., N.A.S., and H.E.S. were supported by NASA LRO/CRaTER/PREDICCS Project (contract NNG11PA03C). We would like to thank MIT PDOS for computing resources and A. Clements for IT assistance. We would like to thank G. A. Neumann, E. Mazarico, and D. E. Smith for their feedback on this paper. LOLA threshold voltage data can be found here: http://imbrium.mit.edu/BROWSE/LOLA_RDR/. The CRaTER data used here are available on the CRaTER website: http://crater-web.sr.unh.edu/. LRO Spice Files can be found here: http://naif.jpl.nasa.gov/pub/naif/pds/data/lro-l-spice-6-v1.0/lrosp_1000/data/spk/. EMMREM data access is provided by the Predictions of radiation from REleASE, EMMREM, and Data Incorporating CRaTER, COSTEP, and other SEP (PREDICCS) measurements (http://prediccs.sr.unh.edu/). NOAA particle flux data are provided by the Space Weather Prediction Center and can be accessed through their archives: http://www.swpc.noaa.gov/Data/

References

Baker, D. (2000), The occurrence of operational anomalies in spacecraft and their relationship to space weather, *IEEE Trans. Plasma Sci.*, *28*(6), 2007–2016.

Barker, M., X. Sun, E. Mazarico, G. Neumann, D. Smith, and M. Zuber (2015a), Lunar phase function in the near-infrared with the lunar orbiter laser altimeter, paper presented at 46th Lunar and Planetary Science Conference, p. 1493, The Woodlands, Tex., 16–20 Mar.

Barker, M., X. Sun, E. Mazarico, G. Neumann, M. Zuber, and D. Smith (2015b), Lunar phase function at 1064 nm from Lunar Orbiter Laser Altimeter passive and active radiometry, *Icarus*, *273*, 96–113.

Chin, G., et al. (2007), Lunar Reconnaissance Orbiter overview: The instrument suite and mission, *Space Sci. Rev.*, *129*(4), 391–419.

Hastings, D. E., and H. B. Garrett (1996), *Spacecraft-Environment Interactions*, Cambridge Univ. Press, Cambridge, U. K.

Kruglanski, M. (2015), SPENVIS Project Manager, BIRA-IASB, Ringlaan 3, B-1180.

Laforce, F. (2009), Optical receiver using silicon APD for space applications, paper SPIE 7330 presented at Defense, Security, and Sensing, International Society for Optics and Photonics, Orlando, Fla., 13 Apr.

Mazarico, E., D. Rowlands, G. Neumann, D. Smith, M. Torrence, F. Lemoine, and M. Zuber (2012), Orbit determination of the lunar reconnaissance orbiter, *J. Geod.*, *86*(3), 193–207.

Mazur, J., W. Crain, M. Looper, D. Mabry, J. Blake, A. Case, M. Golightly, J. Kasper, and H. Spence (2011), New measurements of total ionizing dose in the lunar environment, *Space Weather*, *9*, S07002, doi:10.1029/2010SW000641.

McGarry, J. F., L. K. Pacini, J. B. Abshire, and J. B. Blair (1991), Design and performance of an autonomous tracking system for the Mars Observer Laser Altimeter receiver, paper CThR27 presented at Conference on Lasers and Electro-Optics, Opt. Soc. of Am., Washington, D. C.

Ramos-Izquierdo, L. (2007), LOLA aft-optics instrument delivery review, Delivery Review Presentation.

Ramos-Izquierdo, L., et al. (2009), Optical system design and integration of the Lunar Orbiter Laser Altimeter, *Appl. Opt.*, *48*(16), 3035–3049.

Schwadron, N., et al. (2010), Earth-moon-mars radiation environment module framework, *Space Weather*, *8*, S00E02, doi:10.1029/2009SW000523.

Schwadron, N., et al. (2012), Lunar radiation environment and space weathering from the Cosmic Ray Telescope for the Effects of Radiation (CRaTER), *J. Geophys. Res.*, *117*, E00H13, doi:10.1029/2011JE003978.

Smith, D. E., et al. (2001), Mars Orbiter Laser Altimeter: Experiment summary after the first year of global mapping of Mars, *J. Geophys. Res.*, *106*(E10), 23,689–23,722.

Smith, D. E., et al. (2010), The lunar orbiter laser altimeter investigation on the lunar reconnaissance orbiter mission, *Space Sci. Rev.*, *150*(1–4), 209–241.

Spence, H., et al. (2010), CRaTER: The cosmic ray telescope for the effects of radiation experiment on the lunar reconnaissance orbiter mission, *Space Sci. Rev.*, *150*, 243–284.

Spence, H. E., M. J. Golightly, C. J. Joyce, M. D. Looper, N. A. Schwadron, S. S. Smith, L. W. Townsend, J. Wilson, and C. Zeitlin (2013), Relative contributions of galactic cosmic rays and lunar proton albedo to dose and dose rates near the Moon, *Space Weather*, *11*, 643–650, doi:10.1002/2013SW000995.

Sun, X., and G. Neumann (2015), Calibration of the Mercury Laser Altimeter on the MESSENGER Spacecraft, *IEEE Trans. Geosci. Remote Sens.*, *53*(5), 2860–2874.

Sun, X., D. Reusser, H. Dautet, and J. B. Abshire (1997), Measurement of proton radiation damage to Si avalanche photodiodes, *IEEE Trans. Electron Devices*, *44*(12), 2160–2166.

Sun, X., M. A. Krainak, J. B. Abshire, J. D. Spinhirne, C. Trottier, M. Davies, H. Dautet, G. R. Allan, A. T. Lukemire, and J. C. Vandiver (2004), Space-qualified silicon avalanche-photodiode single-photon-counting modules, *J. Mod. Opt.*, *51*(9–10), 1333–1350.

Sun, X., J. B. Abshire, J. F. McGarry, G. Neumann, J. C. Smith, J. F. Cavanaugh, D. J. Smith, H. J. Zwally, D. E. Smith, and M. T. Zuber (2013), Space lidar developed at the NASA Goddard Space Flight Center—The first 20 years, *IEEE J. Sel. Top. Appl. Earth Obs. Remote Sens.*, *6*(3), 1660–1675.

Tavernier, S. (2010), *Experimental Techniques in Nuclear and Particle Physics*, chap. 2: Interactions of Charged Particles with Matter, pp. 227–275, Springer, Berlin.

Webb, D. F., and J. H. Allen (2004), Spacecraft and ground anomalies related to the October–November 2003 solar activity, *Space Weather*, *2*, S03008, doi:10.1029/2004SW000075.

Wegrzecka, I., M. Wegrzecki, M. Grynglas, J. Bar, A. Uszynski, R. Grodecki, P. Grabiec, S. Krzeminski, and T. Budzynski (2004), Design and properties of silicon avalanche photodiodes, *Opto-Electron. Rev.*, *12*(1), 95–104.